Environmental Microbiology (2007) **9**(11), 2720–2727 doi:10.1111/j.1462-2920.2007.01384.x

Resource dynamics during infection of *Micromonas pusilla* by virus MpV-Sp1

Christopher M. Brown,[1] Douglas A. Campbell[2] and Janice E. Lawrence[1]*

[1]*Biology, University of New Brunswick, P.O. Bag Service 45111, Fredericton NB, Canada E3B 6E1.*

[2]*Biology, Mount Allison University, 63B York Street, Sackville NB, Canada E4L 1G7.*

Summary

Viruses infecting marine phytoplankton drive phytoplankton diversity, terminate blooms and shuttle genetic material. Assessments of the scale of viral impacts on trophic networks are, however, speculative. We investigated fluxes of DNA between host and virus during infection of the prasinophyte alga *Micromonas pusilla* by phycodnavirus MpV SP1. Under a light–dark regimen, viral genomes accumulated to a transient peak within 24 h, at the expense of both host DNA synthesis and nuclear DNA. Viral genome abundance then declined soon after host lysis. This release of a phosphate-rich nucleotide pool during viral infection of phytoplankton should be considered in trophic models. Lysis required light and was stalled in darkness, meanwhile viral genome replication proceeded slowly in the dark. Viral exploitation of this host is therefore only partially light-dependent and infected phytoplankton are poised to lyse at dawn or if mixed to the photic zone. The chloroplast genome remained intact until lysis, indicating that either this DNA pool is inaccessible or the virus spares the chloroplast for its energy and reductant generation. The photochemical turnover of residual Photosystem II complexes accelerated during lysis, indicating that events in late infection heighten demands on the remaining host photosynthetic systems, consistent with the light dependency of lysis.

Introduction

Phytoplankton are important components of global carbon cycling, accounting for nearly half of global annual primary production through their oxygenic photosynthesis (Falkowski and Raven, 1997; Field *et al*., 1998). Removal of phytoplankton cells from marine trophic webs can occur through grazing by heterotrophic zooplankton, sinking into the deep ocean, or lysis due to a variety of mortality mechanisms, including viruses (Bidle and Falkowski, 2004).

Lytic viruses are abundant in marine pelagic systems and viral infection influences phytoplankton growth dynamics and community structure (Bratbak *et al*., 1993; Fuhrman, 1999; Gobler *et al*., 2004), but quantifying the importance of viruses as mortality agents has proven elusive, particularly outside of bloom scenarios. In laboratory cultures, lysis accelerates the release of dissolved organic matter (DOM) from cells into the water (Gobler *et al*., 1997). Estimates of mortality in the field, based on the proportion of phytoplankton that are visibly infected, suggest that viruses channel between 6% and 26% of photosynthetically fixed carbon to the DOM pool (Wilhelm and Suttle, 1999), potentially enlarging the microbial loop at the expense of the grazing loop (Fuhrman, 1999). Large-scale processes such as carbon sequestration into the deep ocean by the biogenic carbon pump may also be pre-empted by viral infection and lysis of large phytoplankton near the surface. In parallel with carbon, other resources including phosphate-rich nucleotides are mobilized from host pools through viral infection and subsequent host lysis.

In host : virus interactions, energy is required to convert host resources into new virus particles. The processes by which viruses subvert and redirect host resources vary, even among closely related viruses. Host physiology can influence the rate and yield of viral multiplication in heterotrophic bacteria (Hadas *et al*., 1997) and in both prokaryotic (Mackenzie and Haselkorn, 1972; Wilson *et al*., 1996) and eukaryotic phytoplankton (Bratbak *et al*., 1993; 1998). The relationship between viruses and photoautotrophic hosts is unique in that light energy provides the energy and reducing power required for net growth of the host. Light may thus also alter infection dynamics and viral multiplication trajectories.

The presence of core Photosystem II genes in the genomes of viruses that infect cyanobacteria (Mann *et al*., 2003) suggests that maintenance of photosynthesis in some instances enables or enhances viral propagation. In cyanobacteria, viral multiplication shows varying levels of light dependence. Light-independent viral multiplication

Received 5 April, 2007; accepted 27 May, 2007. *For correspondence. E-mail jlawrenc@unb.ca; Tel. (+1) 506 458 7842; Fax (+1) 506 453 3583.

was reported for LPP-1 infection of the filamentous cyanobacterium *Phormidium uncinatum*, although the length of the latent period from infection to first appearance of extracellular virus doubled with dark incubation. Energy and reductant were presumably derived from respiration of reserve glycogen (Bisen *et al*., 1988). In contrast, production of SM-1 virus in the single-celled cyanobacterium *Synechococcus cedorum* is inhibited completely by darkness or DCMU (Mackenzie and Haselkorn, 1972).

In *Anacystis nidulans* infected with virus AS-1, virus production was completely inhibited in the dark. DCMU, however, only partially inhibited virus yield (Allen and Hutchison, 1976), suggesting a requirement for ATP production which can be met in part through cyclic electron flow. Assembly of complete virus particles was clearly independent of CO_2 fixation, although the extent of the contribution of reductant and CO_2 fixation to the virus yield could not be concluded by the experiments.

In the cyanobacterium *Plectonema boryanum*, photosynthetic oxygen evolution continued throughout viral infection while respiration increased (Wu and Shugarman, 1967). CO_2 photoassimilation, meanwhile, ceased early in the infection (Ginzburg *et al*., 1968), in a light-dependent manner.

In eukaryotic phytoplankton, the dependence of viral multiplication on host physiology also varies from host to host and among viruses, although there is evidence for light independence in many of the host:virus pairs studied. During infection of the raphidophyte *Heterosigma akashiwo* by a ssRNA virus, HaRNAV, and by two different dsDNA viruses, WBs1 and OIs1, photosynthesis was gradually impaired, as indicated by chlorophyll *a* fluorescence, PSII quantum yield and PSI–PSII electron transport (Juneau *et al*., 2003). Cell lysis by each of these viruses occurred at the same time after infection in either the light or the dark. Despite the apparent independence from photosynthesis, chloroplasts remained intact, at least superficially, until lysis. *Chlorella* NC64A infection by the dsDNA virus PBCV-1 is completely independent of photosynthesis. Rapid suppression of photosynthesis and inhibition of host DNA replication (Van Etten *et al*., 1983) are followed by host nuclear and chloroplast DNA degradation.

Micromonas pusilla is a small (1.5–3.0 μm) prasinophyte algae occurring in both nearshore and oceanic environments (Butcher, 1952). When *M. pusilla* is infected by virus MpV (Mayer and Taylor, 1979), a gradual decline in photosynthetic CO_2 fixation occurs (Waters and Chan, 1982). Light dependency of viral production in *M. pusilla* has not, however, been demonstrated, nor have the effects of infection on photosynthesis and resource pools been measured.

We examined the interaction between *M. pusilla* CCMP 491 and the Prasinovirus type species, dsDNA MpV SP1 (Cottrell and Suttle, 1991). Photosynthetic function and the integrity of the key biochemical complexes, Rubisco, Photosystems I and II, and ATP synthase, were monitored during infection. In parallel we compared infection dynamics and the nucleotide flux from host genomic DNA to viral genomes, under a light–dark regimen and under prolonged darkness. Finally, we sought to identify and describe discrete phases in host genome loss and viral genome accumulation, as the nucleotides harvested from host genomic DNA for incorporation into viral genomes may be a key resource limiting the production of viral particles to sustain transmission of infections through phytoplankton populations (Brown *et al*., 2006).

Results

Growth of cultures

The growth rate (μ) of *M. pusilla* cultures, measured by either chlorophyll autofluorescence (Fig. 1A) or direct cell counts, was between 0.54 and 0.73 day^{-1} at the start of all experiments.

Infection under a light–dark regimen

Infected cultures incubated with a 14 h light : 10 h dark regimen were completely lysed within 48 h. A decline in *in vivo* fluorescence, beginning at approximately 20 h post infection, served as an indicator of cell lysis (Fig. 1A). In cultures late in lysis, microscopic examination confirmed a near complete absence of intact *Micromonas* cells. In contrast, uninfected control cultures showed ongoing growth, primarily during light phases.

The number of viral genomes, as indicated by quantitative polymerase chain reaction (qPCR) of the SP1 virus *dnapol* sequence, increased sharply to a maximum within 24 h (Fig. 1B). A decline in the number of viral genomes accompanied lysis and was followed by a subsequent more gradual decrease, presumably related to decay of viral particles in the media. Control (uninfected) samples from each control culture were run alongside infected culture samples. We did not observe amplification of SP1 virus *dnapol* from any control cultures, indicating that the cultures were free of SP1 virus. We did not plot these zero control points.

In control cells nuclear genomes (18S amplicon) accumulated in parallel with cell growth (note log scale for amplicons, Fig. 1C, versus linear scale for growth, Fig. 1A). Infected cells initially retained their nuclear genomes, but they declined rapidly after 18 h post infection (Fig. 1C), while chloroplast genomes (*rbcL* amplicon) persisted into lysis (Fig. 1D), suggesting that nuclear DNA is preferentially harvested for virus synthesis.

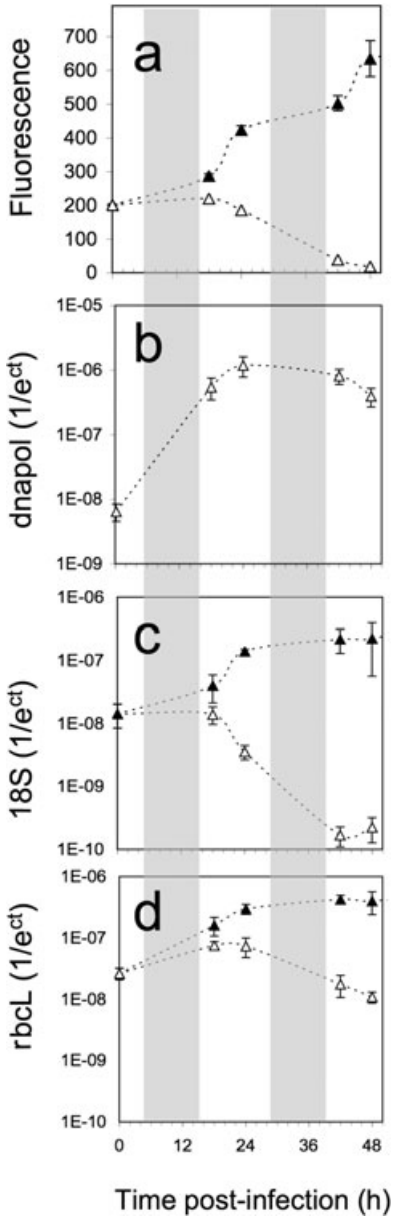

Fig. 1. Viral infection dynamics under 14 h light : 10 h dark incubation. Grey bars indicate 10 h dark periods. Filled symbols, control; open symbols, infected.
A. Growth or decline of cultures monitored by chlorophyll fluorescence, plotted on a linear *y*-axis.
B–D. Quantitative polymerase chain reaction was used to track loci representing (B) viral genome (*dnapol*); (C) nuclear genome (18S); (D) chloroplast genome (*rbcL*), all plotted on log10 *y*-axes. See *Experimental procedures* for an explanation of axis units.
Error bars show one standard deviation. $n = 3$.

To compare resource allocations, rather than genome copies, Fig. 2 shows viral and host nuclear DNA abundances plotted as phosphate equivalents on a linear scale, after correcting for their respective genome sizes: 2×10^5 bp for MpV SP1 (Waters and Chan, 1982) and 2.5×10^7 for *M. pusilla* (Veldhuis *et al.*, 1997). A further correction was made for the estimated four copies of the 18S sequence in the *M. pusilla* genome (Zhu *et al.*, 2005). We noted four discrete phases in the flux of DNA from the host pool through the viral pool to the environment (Fig. 2). In the first phase from infection to 18 h, an increase in viral DNA occurred with no net decline in the nuclear DNA of the infected host cells. Note this initial phase of viral accumulation coincided largely with a 10 h dark phase. In contrast, over this first phase of 0–18 h the uninfected control cells showed significant accumulation of nuclear DNA, which was apparently pre-empted by the viral DNA accumulation in the infected host cells. In the second phase from 18 to 24 h, the onset of the light phase was followed by a sharp drop in host nuclear DNA content that coincided with a further increase in viral genome abundance. A third phase from 24 h onwards showed viral genome abundance declining as cultures began to lyse. A final, slower decline in viral genomes from 48 h onwards (data not shown), presumably associated with viral decay in the culture medium, then followed.

Infection under prolonged darkness

When cultures were incubated in complete darkness for 65 h following infection, lysis of infected cultures and growth of control cultures were both inhibited (Fig. 3A). Return of the cultures to the light–dark regimen allowed the resumption of lysis or growth. Lysis was complete at 114 h, approximately 48 h after the return to the light–dark regimen.

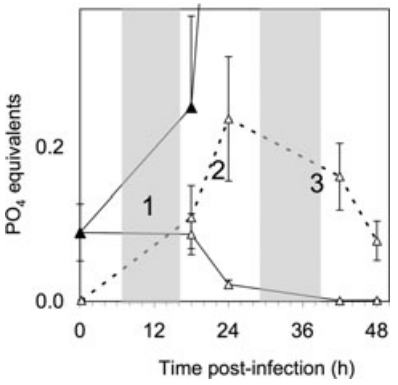

Fig. 2. Mobilization of nucleotide phosphate pools during viral infection. Grey bars indicate 10 h dark periods. Broken line, open symbols – viral nucleotide pool; solid line, open symbols – nuclear nucleotide pool in infected host cells; solid line, filled symbols – nuclear nucleotide pool in control cells. Nucleotide phosphate equivalents were estimated as described in the text. Phases in nucleotide flux: 1, initial viral accumulation without net loss of infected host DNA, note that uninfected control cells show an equivalent accumulation in nuclear DNA pool over the same period; 2, continued viral accumulation to pre-lysis peak with concomitant degradation of host DNA; 3, decline in viral pool following lysis. See *Experimental procedures* for an explanation of axis units. Error bars show one standard deviation. $n = 3$.

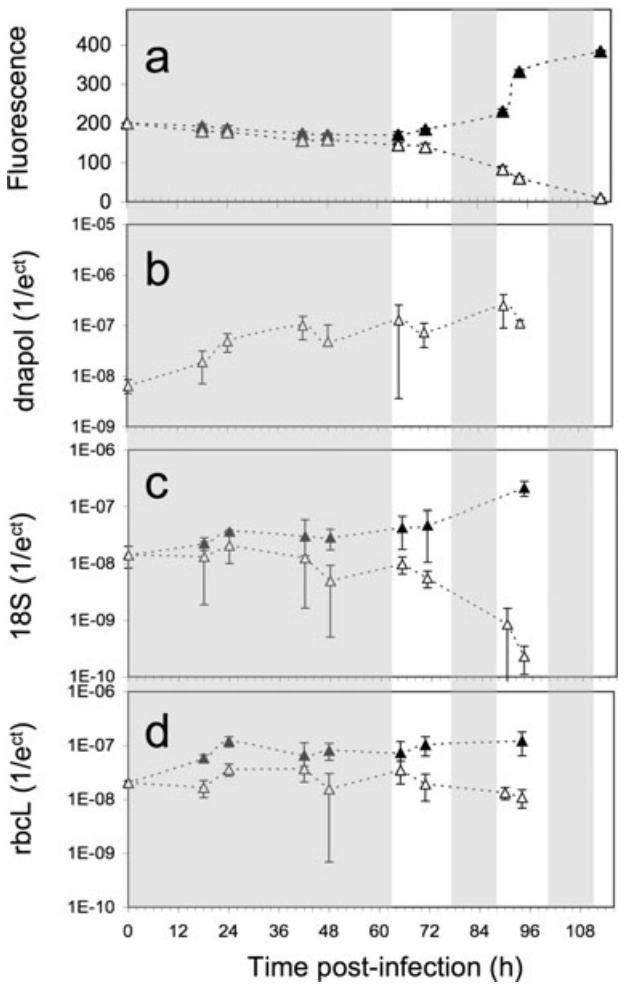

Fig. 3. Viral infection under prolonged darkness. Grey bars indicate dark periods. Filled symbols, control; open symbols, infected.
A. Growth or decline of cultures monitored by chlorophyll fluorescence, plotted on a linear *y*-axis.
B–D. Quantitative polymerase chain reaction was used to track loci representing (B) viral genome (*dnapol*); (C) nuclear genome (18S); (D) chloroplast genome (*rbcL*), all plotted on log10 *y*-axes.
Error bars show one standard deviation. $n = 3$.

While lysis was stalled in the dark, the abundance of viral genomes increased in infected cultures, though at a slower rate and to a lower maximum abundance than under light–dark incubation (Fig. 3B).

Nuclear DNA (18S amplicon) was not degraded in infected cultures in the dark, but the slow accumulation of nuclear genomes seen in dark control cultures was pre-empted by viral infection (Fig. 3C). This supports the pattern observed on a more compressed time scale in Figs 1 and 2. A return to the light–dark growth at 65 h resulted in a rapid loss of nuclear DNA in infected cultures. The chloroplast DNA (*rbcL* amplicon) was steady during the dark phase, and declined only slightly in chloroplast DNA upon return to light–dark incubation (Fig. 3D).

Photosynthetic complexes and oxygen evolution

The absolute levels of four representative photosynthetic protein subunits were determined using quantitative immunoblots (see Fig. 4A). From these we inferred the abundance of key photosynthetic complexes: PsbA for Photosystem II (Fig. 4B), PsaC for Photosystem I (Fig. 4C), RbcL for Rubisco (Fig. 4D) and AtpB for ATP synthase (Fig. 4E).

At 9 h post infection, prior to the onset of lysis, the levels of Rubisco, PSI, PSII or ATP synthase were the same in control and infected cultures (Fig. 4). By 26 h post infection, levels of all four complexes in the infected cultures had fallen as cells entered lysis, but had increased in control cultures in parallel with growth. In spite of this drop, there were no differences in the ratios of key subunits between control and infected cultures at either 9 h or 26 h (Fig. 5). Moreover, these ratios remained steady across the time-course in both control and infected cultures.

The maximum rate of gross photosynthetic oxygen evolution, measured under saturating light and expressed on either a chlorophyll *a* (Fig. 6A) or culture volume basis (data not shown), declined as infected cultures entered into lysis. Oxygen evolution per PSII (taking PsbA as a proxy), however, increased during lysis (Fig. 6B), suggesting that the remaining photosystems were functioning with a higher biochemical turnover rate at this stage in the lytic cycle. A similar pattern was found for oxygen evolution measured at the growth light (85 μmol photons m^{-2} h^{-1}; data not shown).

Discussion

Infection of *M. pusilla* with virus MpV SP1 under a light–dark regimen led to a rapid lysis of most or all phytoplankton cells. The persistence of chloroplast DNA into lysis, several hours beyond the point at which nuclear DNA declined in abundance, can be interpreted in several ways. Bearing in mind that the presence of superficially intact chloroplasts cannot alone be taken to indicate a utility for or a dependence on photosynthesis for the lytic cycle, chloroplasts may simply be a recalcitrant pool of resources that are left untapped by the virus. Alternatively, the chloroplast may be important as a source of energy and reductant for infection of *M. pusilla* by MpV SP1. Given that the nucleotides in a single chloroplast genome, fully broken down, would only account for approximately one new viral genome, the benefits of plundering this organelle for nucleotides would be low in the context of production of a total viral burst of 70–100 particles per cell (Waters and Chan, 1982).

The maintenance of the photosynthetic apparatus and the stability in the ratios of several key photosynthetic

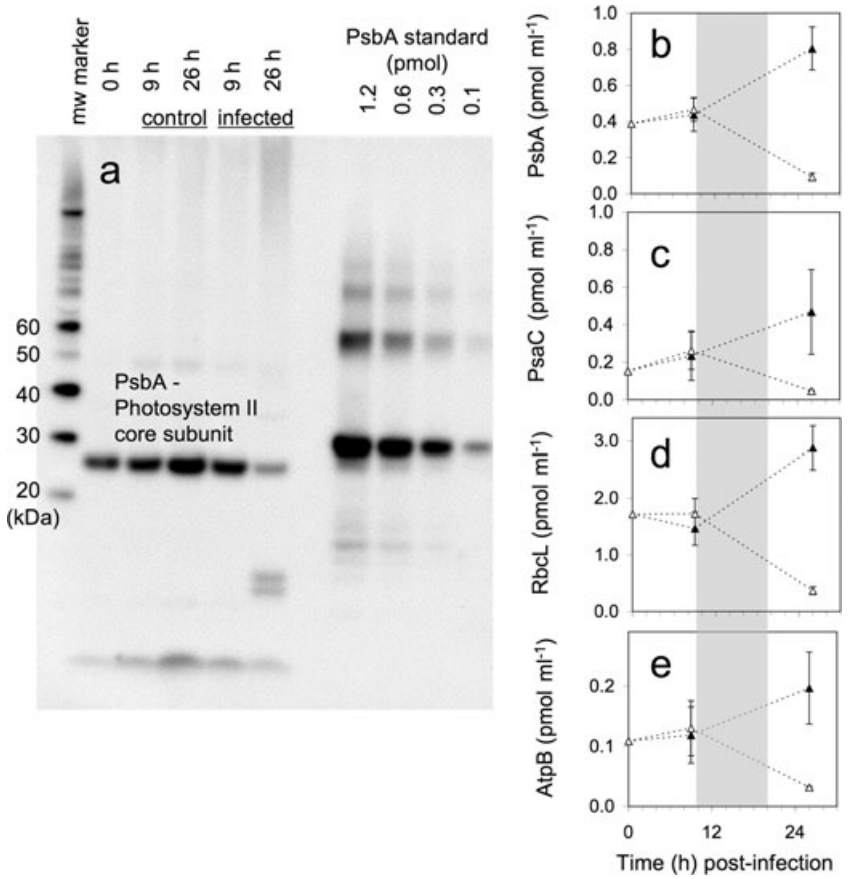

Fig. 4. Quantitative immunodetections of key photosynthetic proteins.
A. Example blot, showing PsbA quantification. Samples were loaded on an equal culture volume basis.
B–E. Grey bar indicates dark period. Closed symbols, control; open symbols, infected. Subunit quantities (pmol subunit per ml culture) of (B) PsbA, (C) PsaC, (D) RbcL and (E) AtpB in cultures.
Error bars show one standard deviation. $n = 3$.

proteins until lysis show that the chloroplast integrity during MpV SP1 infection goes well beyond superficial. Moreover, continued oxygen evolution into early infection and an enhanced rate of oxygen evolution per remaining Photosystem II during lysis argues that photosynthesis serves viral demands through the infection, and in particular during late infection or lysis.

Dark incubation of infected *M. pusilla* demonstrated an uncoupling of viral replication from lysis. Lysis was stalled in the dark, while accumulation of viral genomes proceeded, although more slowly in dark than in light–dark-incubated cultures. Sufficient energy and possibly reductant could be derived from stored metabolic intermediates to allow this slow accumulation of viral genomes, apparently at the expense of host DNA replication, as suggested by comparison of the dark accumulation of host nuclear DNA in uninfected control cells with dark accumulation of viral DNA in infected host cells. DNA synthesis from pre-formed nucleic acids would require primarily ATP, while *de novo* synthesis would consume both reductant and ATP. Cells in the dark may be primed for completion of the lytic cycle upon return to the light. Placing this finding in an ecological context, maintaining viral genome replication in the dark would allow infection to proceed as cells cycled between the euphotic and the aphotic zone, or from night to day. Mechanistically the oxygen evolution data show that late infection and lysis place heavy demands on the remaining photosynthetic metabolism, perhaps to drive capsid accumulation or assembly. This may account for the light requirement for lysis in comparison with the partial independence of viral genome replication from light.

The flux of nucleic acids out of the host genome pool and into the viral genome pool showed an interesting multiphasic pattern. An initial accumulation of viral genomes took place prior to the rapid decline of host nuclear genome copy number, while the final increase in viral genome abundance corresponded to the breakdown of host nuclear DNA. The changes in these two pools appears to be roughly equal in magnitude and opposite in direction. Our results on viral genome abundance in these experiments are consistent with the hypothesis that viral production is constrained by host DNA content, as proposed in Brown and colleagues (2006).

A sharp but limited drop in viral genomes upon the start of lysis suggests that the host contains unpackaged copies of viral DNA, possibly because an excess of viral genomes is synthesized. One plausible explanation for this sudden decline is that an excess of genomes is needed to create a thermodynamic state favourable for

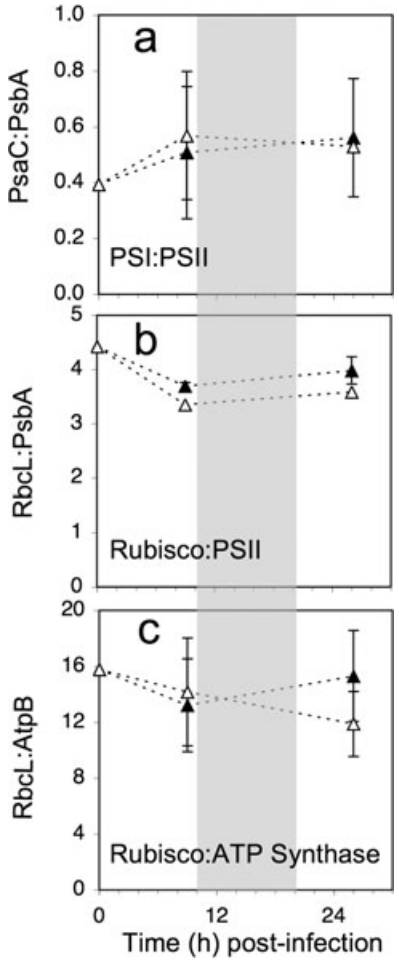

Fig. 5. Molar ratios of key photosynthetic protein subunits. Closed symbols, control; open symbols, infected. Error bars show one standard deviation. $n = 3$.

the rapid packaging of genomes. Some viruses assemble spontaneously once constituents have reached a critical level (see, for example, Rapaport, 2004). While such models focus on the protein capsid, the packaging of genomes into capsids may be similarly influenced by the energy landscape. Moreover, in order for the viral genome to be packaged into icosahedral capsids, the genome may serve as a nucleation centre for spontaneous assembly.

An alternative explanation is that this excess may represent a substantial pool of complete, but structurally defective viruses. These would be rapidly degraded upon exposure to the lurking heterotrophic opportunists in the medium.

Finally, it is possible that the rapid loss of viral genomes reflects an imbalance between the number of genomes and the number of capsids available to house them. We did not measure capsid proteins in this study, so we cannot rule this out. Further experiments in which both capsid protein and DNA were tracked would be informative, as would growth of cultures in medium with different N : P ratios. While the N : P ratio of nutrient replete microalgae is typically between 15 and 30 (Geider and La Roche, 2002), N : P of DNA is less than 5.

In any of these scenarios, the release of phosphate-rich DOM, in the form of nucleotides, into the surrounding media is a consideration in models of matter and energy cycling from phytoplankton to the wider aquatic system. The nature and flux of released organic matter shapes the interaction between top-down (viral infection) and bottom-up (nutrients) factors acting upon phytoplankton communities (Raven, 2006).

Experimental procedures

Organisms and culturing

Micromonas pusilla CCMP 491 was cultured at 20°C in 100 ml of F/2 media (Guillard, 1975) prepared with filtered seawater. Cultures were not axenic and contained a heterotrophic bacteria community that peaked in density following lysis of phytoplankton cells (data not shown). Cultures were illuminated under 85 μmol m^{-2} s^{-1} light, with a 14 h light : 10 h dark regimen. For prolonged dark incubations, flasks were covered with aluminum foil and sampled in a dark room under dim green light.

Exponential cultures were infected in the middle of the light phase by adding 1% (v/v) cleared lysate from an MpV SP1-infected *M. pusilla* culture, which is sufficient to produce a one-step viral growth experiment, indicating that all the cells

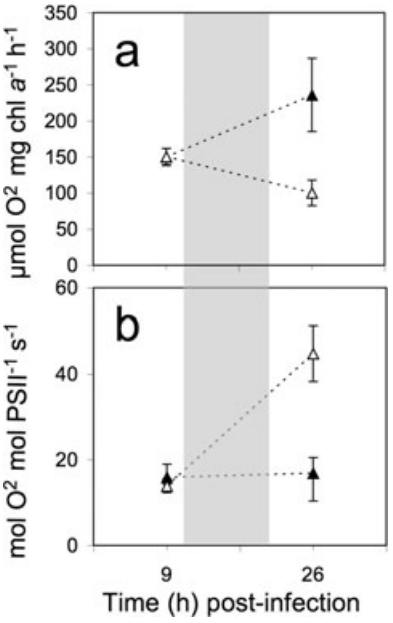

Fig. 6. Photosynthesis during infection. Maximum rates of gross O_2 evolution (corrected for dark respiration) at saturating light (850 μmol photons m^{-2} s^{-1}). Error bars show one standard deviation. $n = 3$.

were initially infected. Adding more virus does not decrease the period of time until complete culture lysis. One per cent (v/v) is thus a titre that produces a one-step viral growth experiment (Ellis and Delbruck, 1939; Nagasaki *et al*., 1999; Thyrhaug *et al*., 2002). Nonetheless, starting viral genomes were at least two orders of magnitude lower than the peak level accumulated just before lysis (Fig. 1B), corresponding to a viral burst size of *c*. 100 viral genomes per host cell. Because of the very small size of *M. pusilla* and the presence of cell debris, organelles and heterotrophic cells in lysing cultures, cell counts can only be accomplished using fluorescence microscopy. In stressed and lysing *Micromonas* cells, the fluorescence signal bleaches rapidly, making such cell counts of questionable value in any quantitative sense. We and others (Mayer, 1978) have instead established that fluorescence is a reliable proxy for *Micromonas* cell number and cell integrity. Therefore, growth of cultures was monitored by chlorophyll fluorescence (Turner Designs TD-700 benchtop fluorometer), with validation of complete cell lysis by direct counts [Improved Neubauer counting chamber under epifluorescence microscopy (Leica)].

Tracking viral, host nuclear and chloroplast DNA

Strain-specific primers were designed for real-time qPCR of the SP1 viral DNA polymerase gene (*dnapol*), *dnapol* forward tatggaaatgttccgggtgtca; *dnapol* reverse accgtaaacggagttcatcg; the *M. pusilla* gene for the chloroplast-encoded large subunit of Rubisco (*rbcL*), *rbcL* forward atcgcgtacattgcttaccc; *rbcL* reverse acatccaaggagaccacgtc; and the nuclear 18S rDNA gene, 18S forward atggccgttcttagttggtgg; 18S reverse ctcgttgcattcgtcagtgt. All primers had melting temperatures of 58–61°C and generated short amplicons (200–300 bp). Culture samples (200 μl) were removed at time points and stored at –20°C. Prior to performing qPCR, 50 μl of culture to be analysed was diluted fivefold in distilled, deionized H_2O and flash frozen in liquid N_2. Samples were thawed and vortexed well to suspend and distribute cells evenly. For amplification of *rbcL* and 18S sequences, 5 μl of these diluted samples were used. For *dnapol*, 1 μl of diluted sample was used. Experiments were conducted in triplicate, and individual qPCR reactions were prepared in duplicate. For each sample, we calculated $1/e^{C_t}$, which is representative of the copy number of the original template in the sample (Heid *et al*., 1996), as follows: the average PCR efficiency (*e*) for each primer pair was determined in the early exponential phase of the qPCR reaction (Linreg software). This efficiency value (*e*) was raised to the power C_t (cycle threshold) which is the PCR cycle at which the intensity of the fluorescence from SYBR green in the reaction rises above background to cross a threshold level (ABI PRISM literature; Applied Biosystems, Foster City, CA, USA).

Photosynthetic oxygen evolution

Oxygen evolution was measured with a liquid phase silver electrode (Hansatech). Chlorophyll was measured by centrifuging 2 ml of culture for 5 min at 10 000 *g*, extracting the pellet in 80% (v/v) acetone, and reading the absorbance of the extract at 664 and 647 nm (Porra, 2002). Net oxygen evolution was measured at the growth light and at saturating light and corrected for dark respiration to estimate gross photosynthetic rates.

Quantitative protein immunodetection

Ten millilitres of culture was removed and centrifuged for 15 min at 4000 *g* in 15 ml plastic centrifuge tubes. Nine millilitres of medium was removed and cells were transferred to 1.5 ml microfuge tubes, which were centrifuged for 5 min at 10 000 *g*. All medium was removed and pellets were frozen at –20°C until further processing. Disruption of cells and extraction of proteins was performed by a combination of sonication and freeze/thaw, as described in C.M. Brown, J.D. MacKinnon, A.M. Cockshutt, T.A. Villareal, D. Durnford, and D.A. Campbell (submitted). Total protein was measured on lysates using a modified detergent compatible Lowry (Bio-Rad). Chlorophyll content was determined by diluting 50 μl of extract in 950 μl of 80% (v/v) acetone, incubating at –20°C for 15 min, centrifuging for 2 min at 10 000 *g* and reading the absorbance at 664 and 647 nm (Porra, 2002). Equal culture volume equivalents (667 μl) were loaded on BisTris polyacrylamide gels (Invitrogen). Known quantities of recombinant protein standards (Agrisera, Ab), loaded in wells adjacent to samples, allowed us to calibrate detections and determine absolute quantities of each subunit.

Proteins were detected using primary antibodies towards RbcL, PsbA, PsaC and AtpB (Agrisera Ab). After incubation with HRP-conjugated secondary antibodies, blots were developed with ECL Advance (GE Healthcare) and signal intensity was measured using a FluorSmax imager (Bio-Rad).

Acknowledgements

This work was supported by grants from the Natural Science and Engineering Research Council of Canada (NSERC), the Canada Foundation for Innovation (CFI) and the New Brunswick Innovation Foundation (NBIF). We thank Dion Durnford, Vanessa Paesani, Christophe Six and Amanda Cockshutt for assistance and discussions.

References

Allen, M.M., and Hutchison, F. (1976) Effect of some environmental factors on cyanophage AS-1 development in *Anacystis nidulans*. *Arch Microbiol* **110:** 55–60.

Bidle, K.D., and Falkowski, P.G. (2004) Cell death in planktonic, photosynthetic microorganisms. *Nat Rev Microbiol* **2:** 643–655.

Bisen, P.S., Audholia, S., Shukla, H.D., Gupta, A., and Singh, D.P. (1988) Evidence for photosynthetic independence of viral multiplication in cyanophage LPP-1 infected cyanobacterium *Phormidium uncinatum*. *FEMS Microbiol Lett* **52:** 225–228.

Bratbak, G., Egge, J.K., and Heldal, M. (1993) Viral mortality of the marine alga *Emiliania huxleyi* (*Haptophyceae*) and termination of algal blooms. *Mar Ecol Prog Ser* **93:** 39–48.

Bratbak, G., Jacobsen, A., Heldal, M., Nagasaki, K., and Thingstad, F. (1998) Virus production in *Phaeocystis pouchetii* and its relation to host cell growth and nutrition. *Aquat Microb Ecol* **16:** 1–9.

Brown, C.M., Lawrence, J.E., and Campbell, D.A. (2006) Are phytoplankton population density maxima predictable through analysis of host and viral genomic DNA content? *J Mar Biol Assoc UK* **86:** 491–498.

Butcher, R. (1952) Contributions to our knowledge of the smaller marine algae. *J Mar Biol Assoc UK* **31:** 175–191.

Cottrell, M.T., and Suttle, C.A. (1991) Wide-spread occurrence and clonal variation in viruses which cause lysis of a cosmopolitan, eukaryotic marine phytoplankter, *Micromonas pusilla*. *Mar Ecol Prog Ser* **78:** 1–9.

Ellis, E.L., and Delbruck, M. (1939) The growth of bacteriophage. *J Gen Physiol* **22:** 365–384.

Falkowski, P.G., and Raven, J. (1997) *Aquatic Photosynthesis*. Oxford, UK: Blackwell.

Field, C.B., Behrenfeld, M.J., Randerson, J.T., and Falkowski, P. (1998) Primary production of the biosphere: integrating terrestrial and oceanic components. *Science* **281:** 237–240.

Fuhrman, J.A. (1999) Marine viruses and their biogeochemical and ecological effects. *Nature* **399:** 541–548.

Geider, R.J., and La Roche, J. (2002) Redfield revisited: variability of C : N : P in marine microalgae and its biochemical basis. *Eur J Phycol* **37:** 1–17.

Ginzburg, D., Padan, E., and Shilo, M. (1968) Effect of cyanophage infection on CO_2 photoassimilation in *Plectonema boryanum*. *J Virol* **2:** 695–701.

Gobler, C.J., Hutchins, D.A., Fisher, N.S., Cosper, E.M., and Sanudo-Wilhelmy, S.A. (1997) Release and bioavailabilityof C, N, P, Se, and Fe following viral lysis of a marine chrysophyte. *Limnol Oceanogr* **42:** 1492–1504.

Gobler, C.J., Deonarine, S., Leigh-Bell, J., Gastrich, M.D., Anderson, O.R., and Wilhelm, S.W. (2004) Ecology of phytoplankton communities dominated by *Aureococcus anophagefferens*: the role of viruses, nutrients, and microzooplankton grazing. *Harmful Algae* **3:** 471–483.

Guillard, R.L.L. (1975) Culture of phytoplankton for feeding marine invertebrates. In *Culture of Marine Invertebrate Animals.* Smith, W. L., and Chanley, M.H. (eds). New York, USA: Plenum Press, pp. 26–60.

Hadas, H., Einav, M., Fishov, I., and Zaritsky, A. (1997) Bacteriophage T4 development depends on the physiology of its host *Escherichia coli*. *Microbiology* **143:** 179–185.

Heid, C.A., Stevens, J., Livak, K.J., and Williams, P.M. (1996) Real time quantitative PCR. *Genome Res* **6:** 986–994.

Juneau, P., Lawrence, J.E., Suttle, C.A., and Harrison, P.J. (2003) Effects of viral infection on photosynthetic processes in the bloom-forming alga *Heterosigma akashiwo*. *Aquat Microb Ecol* **31:** 9–17.

Mackenzie, J.J., and Haselkorn, R. (1972) Photosynthesis and the development of blue-green algal virus SM-1. *Virology* **49:** 517–521.

Mann, N.H., Cook, A., Millard, A., Bailey, S., and Clokie, M. (2003) Bacterial photosynthesis genes in a virus. *Nature* **424:** 741.

Mayer, J.A. (1978) Isolation and ultrastructural study of a lytic virus in the small marine photosynthetic phytoflagellate, *Micromonas pusilla* (Prasinophyceae). PhD Thesis. University of British Columbia.

Mayer, J.A., and Taylor, F.J.R. (1979) A virus which lyses the marine nanoflagellate *Micromonas pusilla*. *Nature* **281:** 299–301.

Nagasaki, K., Tarutani, K., and Yamaguchi, M. (1999) Growth characteristics of *Heterosigma akashiwo* virus and its possible use as a microbiological agent for red tide control. *Appl Environ Microbiol* **65:** 898–902.

Porra, R.J. (2002) The chequered history of the development and use of simultaneous equations for the accurate determination of chlorophylls *a* and *b*. *Photosynth Res* **73:** 149–156.

Rapaport, D.C. (2004) Self-assembly of polyhedral shells: a molecular dynamics study. *Phys Rev E Stat Nonlin Soft Matter Phys* **70:** 051905.

Raven, J.A. (2006) Aquatic viruses: the emerging story. *J Mar Biol Assoc UK* **86:** 449–451.

Thyrhaug, R., Larsen, A., Brussaard, C.P.D., and Bratbak, G. (2002) Cell cycle dependent virus production in marine phytoplankton. *J Phycol* **38:** 338–343.

Van Etten, J.L., Burbank, D.E., Xia, Y., and Meints, R.H. (1983) Growth cycle of a virus, PBCV-1, that infects *Chlorella*-like algae. *Virology* **126:** 117–125.

Veldhuis, M.J.W., Cucci, T.L., and Sieraki, M.E. (1997) Cellular DNA content of marine phytoplankton using two new fluorochromes: taxonomic and ecological implications. *J Phycol* **33:** 527–541.

Waters, R.E., and Chan, A.T. (1982) *Micromonas pusilla* virus: the virus growth cycle and associated physiological events within the host cells; host range mutation. *J General Virol* **63:** 199–206.

Wilhelm, S.W., and Suttle, C.A. (1999) Viruses and nutrient cycles in the sea. *BioScience* **49:** 781–788.

Wilson, W.H., Carr, N.G., and Mann, N.H. (1996) The effect of phosphate status on the kinetics of cyanophage infection in the oceanic cyanobacterium *Synechococcus* sp WH7803. *J Phycol* **32:** 506–516.

Wu, J.H., and Shugarman, P.M. (1967) Effect of virus infection on rate of photosynthesis and respiration of a blue-green alga, *Plectonema boryanum*. *Virology* **32:** 166–167.

Zhu, F., Massana, R., Not, F., Marie, D., and Vaulot, D. (2005) Mapping of picoeucaryotes in marine ecosystems with quantitative PCR of the 18S rRNA gene. *FEMS Microbiol Ecol* **52:** 79–92.

